ligands, charge on the complex, geometry of the complex, and ionization of coordinated water have a smaller effect (0.1 ppm) on the C(2)-H resonance of the coordinated imidazole than coordination with about a 0.5 ppm change from imidazolium. C(2)-H exchange was found for coordinated imidazole and *N*-methylimidazole, but the metalated imidazoles exchanged much more slowly than the analogous methylated (10^{-3}) or protonated species.[32] In neutral regions, coordination inhibits exchange but, in basic regions, may enhance exchange depending on the relative concentrations of positive species to metalated species in solution. Using ^{13}C NMR spectroscopy, we have been able to determine that in the 4-methyl complex the quaternary carbon is adjacent to the ionizable H. The histidine in the Co(en)HisHCl$^+$ complex is tridentate with the cis configuration. The information on these model systems should be useful in identifying histidines coordinated to metal in proteins, as well as helping to identify the source of the pH 6-7 ionization in carbonic anhydrase.

Acknowledgment. The authors gratefully acknowledge the financial support of the Petroleum Research Fund, administered by the American Chemical Society, and partial support from Grant RR08016 from the National Institutes of Health. They also thank Jerome Harris and Agnes Nguyenpho for their help with potentiometric titrations.

Registry No. *cis*-Co(en)$_2$(H$_2$O)ImH^{3+}, 71155-64-1; *cis*-Co(en)$_2$(OH)Im$^+$, 88657-79-8; *trans*-Co(en)$_2$(H$_2$O)ImH^{3+}, 88728-25-0; *trans*-Co(en)$_2$(OH)ImH^{2+}, 88728-26-1; *cis*-Co(en)$_2$Cl(*N*-MeIm)$^{2+}$, 60314-39-8; *cis*-Co(en)$_2$(H$_2$O)(*N*-MeIm)$^{3+}$, 60314-42-3; *cis*-Co(en)$_2$(OH)(*N*-MeIm)$^{2+}$, 88657-80-1; *cis*-Co(en)$_2$Cl(4-MeImH)$^{2+}$, 88657-81-2; *cis*-Co(en)$_2$(H$_2$O)(4-MeImH)$^{3+}$, 88657-77-6; *cis*-Co(en)$_2$(OH)(4-MeImH)$^{2+}$, 88657-82-3; [Co(en)(HisH)Cl]Cl, 88657-76-5; Co(en)(HisH)Cl$^+$, 88657-78-7; Co(en)(H$_2$O)HisH^{2+}, 88657-83-4; Co(en)(OH)HisH$^+$, 88657-84-5; ImH, 288-32-4; *cis*-Co(en)$_2$ClImH^{2+}, 60314-38-7.

Supplementary Material Available: Tables of UV-vis spectral data, selected bond lengths and angles, crystal data and parameters of data collection, least-squares planes data, thermal parameters, and structure factor amplitudes (22 pages). Ordering information is given on any current masthead page.

Contribution from LURE,[1a] the Laboratoire de Physicochimie Minérale, and ERA 672, Université de Paris Sud, 91405 Orsay Cedex, France, Laboratoire de Physicochimie Structurale, Université de Paris-Val de Marne, 94000 Creteil, France, Laboratoire de Chimie Minérale I, Université de Paris Sud, 92290 Chatenay Malabry, France, and Istituto Guido Donegani, SpA, 28100 Novara, Italy

Resolution of a Structural Disorder through Apparently Inconsistent X-ray Diffraction and EXAFS Data: Structure of the New Layered System $Mn_{1-x}Cu_{2x}PS_3$ (x = 0.13)

Y. MATHEY,*[1b] A. MICHALOWICZ,[1c] P. TOFFOLI,[1d] and G. VLAIC[1e]

Received May 19, 1983

The synthesis, characterization, and complete structural determination of the layered system $Mn_{0.87}Cu_{0.26}PS_3$ are reported. A room-temperature single-crystal X-ray diffraction (XRD) study and powder EXAFS measurements at the manganese and copper K edges (15 and 300 K spectra) have been performed. XRD shows the existence of disorder and leads to metal-sulfur distances inconsistent with EXAFS data. This puzzling difference has been overcome and has proved very helpful for leading to a detailed picture of the metallic sites. It is shown that besides the classical [S_3PPS_3] entities two distinct types of pseudooctahedra are randomly distributed within the layers: (a) [MnS_6] entities with the expected Mn-S = 2.61 Å distances and (b) [$S_3Cu\cdots CuS_3$] bimetallic entities with center-to-apex distances of 2.83 Å.

Introduction

In recent years, there has been an increasing interest in intercalated layered systems of the MPS_3 family (where M^{II} is a transition-metal ion), which exhibit promising electrical and magnetic properties.[2] The structural versatility of these layer-type systems is well illustrated by $In_{2/3}\square_{1/3}PS_3$ ($\square$ stands for a metal vacancy)[3] and $Cr_{1/2}Cu_{1/2}PS_3$,[4] for which it was established that the occupancy of all the pseudooctahedral intralayer metallic sites was not a strict requirement for the stability of these two-dimensional frameworks.

In other respects, quite high concentrations of intralamellar metallic vacancies were shown to be tolerable by the 2D structure in a series of intercalation compounds $M^{II}_{1-x}\square_xPS_3,2x[C^+]$, where M^{II} is Mn, Zn, and Cd and C^+ represents cationic species like alkali, metallocenium, and ammonium ions.[5] However, no evidence for a superstructure was ever found in the X-ray powder diffraction patterns of these new intercalates.

During the course of our search for ordered intercalated systems, we have prepared several lamellar compounds of general formula $M_{1-x}M'_{2x}PS_3$ with M^{II} = Mn and Cd and where M'^{I} = Cu and Ag monocations were supposed to be distributed in an ordered manner over interlamellar sites. The synthesis, characterization, and complete structural determination of the $Mn_{0.87}Cu_{0.26}PS_3$ compound are reported hereafter.

In the present work, the conjunction of X-ray diffraction (XRD) results with EXAFS data proved to be invaluable; consequently, special emphasis is given to the complementarity of these two techniques.

Experimental Section

Synthesis. When the pure (~99.9%) elements Mn, Cu, P, and S in $^5/_6$:$^2/_6$:1:3 ratios were heated at 750 °C for 2 weeks in evacuated quartz ampules, a polycrystalline powder of $Mn_{1-x}Cu_{2x}PS_3$ with x = 0.13 was obtained. Subsequent treatment by chemical transport led to small green monocrystalline platelets suitable for X-ray dif-

(1) (a) LURE: CNRS laboratory associated with the Université de Paris Sud. (b) Laboratoire de Physicochimie Minérale and ERA 672. (c) Université de Paris-Val de Marne and LURE. (d) Laboratoire de Chimie Minérale I. (e) Istituto Guido Donegani and LURE.
(2) Brec, R.; Schleich, D. M.; Ouvrard, G.; Louisy, A.; Rouxel, J. *Inorg. Chem.* **1979**, *18*, 1814.
(3) (a) Soled, S.; Wold, A. *Mater. Res. Bull.* **1976**, *11*, 657. (b) Diehl, R.; Carpentier, C. D. *Acta Crystallogr., Sect. B: Struct. Crystallogr. Cryst. Chem.* **1978**, *B34*, 1097.
(4) (a) Leblanc, A.; Rouxel, J. *C. R. Seances Acad. Sci., Ser. C* **1980**, *291*, 263. (b) Colombet, P.; Leblanc, A.; Danot, M.; Rouxel, J. *J. Solid State Chem.* **1982**, *41*, 174.
(5) Clement, R. *J. Chem. Soc., Chem. Commun.* **1980**, 647.

0020-1669/84/1323-0897$01.50/0

Table I. Positional and Thermal Parameters in $Mn_{1-x}Cu_{2x}PS_3$ ($\times 10^4$)

	T^a	x	y	z	β_{11}	β_{22}	β_{33}	β_{12}	β_{13}	β_{23}
Mn	0.846 (6)	0	0	3327 (1)	71 (2)	105 (2)	20 (1)	36 (2)		
Cu	0.120 (3)	5736 (6)	2305 (7)	1671 (3)	32 (7)	188 (1)	10 (2)	63 (7)	−2 (3)	−1 (3)
P	1	549 (2)	1686 (2)	0	44 (3)	57 (2)	14 (1)	22 (2)		
S(1)	1	7614 (2)	2504 (2)	0	69 (1)	74 (2)	36 (1)	41 (2)		
S(2)	1	2426 (1)	2532 (1)	1601 (1)	106 (2)	81 (2)	20 (1)	23 (2)	−17 (1)	−6 (1)

[a] Occupancy factor.

fraction analysis as well as for spectroscopic experiments on oriented samples.

X-ray Diffraction Study. Single-crystal Weissenberg studies (Cu Kα) revealed that $Mn_{1-x}Cu_{2x}PS_3$ is monoclinic and belongs to the $B2/m$, $B2$, or Bm space group (first setting of ref 16). Some spots present a broad and diffuse character, and no superstructure could be found. Accurate lattice parameters were determined with an Enraf-Nonius CAD-4 diffractometer using Mo Kα radiation and were found to be a = 6.090 (4) Å, b = 6.815 (4) Å, c = 10.5398 (6) Å, and γ = 107.11 (3)° at 22 °C; the volume of the cell is 418 Å^3, and the calculated density with Z = 4 is 3.04 g cm^{-3}. Intensity data were collected from a hexagonal prismatic crystal of approximate dimensions 0.30 × 0.25 × 0.05 mm with the above-mentioned diffractometer. The intensities of 752 spots were measured in the 0–32° range with use of the 2θ scan technique with $\Delta\theta = 3.3 + 1.4 \tan\theta$. A total of 700 independent reflections with intensities greater than $3\sigma(I)$ were corrected for Lorentz and polarization factors; absorption corrections were performed with a program adapted from de Meulanaer and Tompa.[6] The transmission factors lie in the 0.32–0.78 range with a linear absorption coefficient μ(Mo Kα) = 4.66 mm^{-1}.

EXAFS Data Collection and Analysis. EXAFS spectra of $Mn_{0.83}Cu_{0.26}PS_3$ were recorded at both the manganese and copper K edges (E_0 K-edge values: 6543 and 8992 eV, respectively) on the EXAFS I spectrometer at LURE (the French synchrotron radiation laboratory) described by Raoux et al.[7] Measurements were made at two different temperatures (15 and 300 K) on a thin layer of powdered sample (20 × 5 mm^2, 10 mg at Mn edge, leading to μx = 1.6–2.7 before and after the edge; 20 mg at Cu edge, leading to μx = 2.1–2.6[28]). Pure $MnPS_3$ and $K_2Cu(S_2C_2O_2)_2$, whose spectra were previously recorded,[8,9] were also used in this work as model compounds with known metal–sulfur distances.

The data analysis was carried out by following a well-known procedure thoroughly described.[10] It includes (i) data reduction from $\mu(h\nu)$ (linear X-ray absorption coefficient vs. the photon energy) to $k[\chi(k)]$, where χ(k) is the EXAFS modulation above the threshold E_0 and k the photoelectron wave vector $k = [(2m_e/\hbar^2)(h\nu - E_0)]^{1/2}$, (ii) Fourier transform of $k^3[\chi(k)]$ to obtain the radial distribution $\tilde{F}(R)$ = FT $\{k^3[\chi(k)]\}$, (iii) Fourier filtering, and (iv) least-squares fitting of the filtered spectra to the standard EXAFS formula

$$k[\chi(k)] = \sum_i \frac{[f_i(k)]N_i}{R_i^2} \sin [2kR_i + \phi_i(k)] e^{-2\sigma_i^2 k^2} e^{-2R_i/\lambda}$$

where N_i represents the number of atoms at a distance R_i from the absorber (Mn or Cu), σ_i is a damping coefficient due to thermal and structural distribution of distances, λ is the mean free path of the photoelectron (an average value of 8 Å has been used in this work), and $f_i(k)$ and $\phi_i(k)$ are the amplitude and phase shift functions (tabulated values of Teo et al.[11] have been used throughout this work). Moreover, the E_0 value was fitted as a variable parameter. The usual accuracy of 0.01–0.02 Å for the determination of R_i depends on the phase shift transferability and was checked on the model compounds. On the other hand, the values obtained for σ_i, which is related to the amplitude of the EXAFS signal, must not be used as absolute structural parameters. They were used in this work only to compare distance mean square deviations in similar environments.[29]

Characterization

Analyses. The composition and the value x = 0.13 of the title compound were established by full elemental analysis and with a CAMEBAX electronic microprobe instrument using Cu_3PS_4 and $MnTiO_3$ as standards. Although there is some scatter among individual values of metallic percentages, these analyses indicate that x = 0.13 and that Mn^{II} vacancies are balanced by $2x$ = 0.26 Cu^I monocations. Nevertheless a slight deviation from the ideal stoichiometry in manganese and/or copper cannot be totally ruled out. Anal. Calcd for $Mn_{1-x}Cu_{2x}PS_3$ with x = 0.13: Mn, 24.96; Cu, 8.63; P, 16.18; S, 50.23. Found by chemical analyses (values averaged over four distinct sets of measurements): Mn, 24.3; Cu, 8.2; P, 16.2; S, 49.6. Found by microprobe on the XRD-investigated single crystal: Mn, 22.3; Cu, 9.3; P, 15.8; S, 52.6.

Physical Measurements. The magnetic susceptibility investigation was performed with use of the Faraday method between 4.2 and 300 K. The χ_M vs. temperature curve strongly recalls the behavior observed in $MnPS_3$ intercalates.[12] The slope of the high-temperature-range linear part of the curve is consistent with the presence of Mn^{II} as the only magnetic centers. XPS and Auger spectra recorded at 240 K on polycrystalline samples of $Mn_{1-x}Cu_{2x}PS_3$ (x = 0.13) also reveal that no Cu^{II} centers are present. The UV–visible (850–200 nm) absorption spectrum compares with those obtained for the $MnPS_3$ layer compound;[2] in agreement with the above susceptibility and XPS results no additional features attributable to d–d transitions arising from possible Cu^{II} centers were detected in the visible range of this electronic spectrum. As far as the vibrational characterization is concerned, it turns out that only a complete IR and Raman study down to very low frequency can provide the basis of a significant comparison with $MnPS_3$. These vibrational characteristics together with conduction and more detailed magnetic properties are described elsewhere.[14]

Structure of $Mn_{0.87}Cu_{0.26}PS_3$

X-ray Diffraction (XRD) Determination of the Structure. The cell parameters of $Mn_{0.87}Cu_{0.26}PS_3$ are closely related to those of $FePS_3$.[15] Therefore, the refinement was carried out in the centrosymmetric space group $B2/m$, giving at first an occupancy probability of 1 to the S, P, and Mn atoms on the S, P, and Fe positions of the model structure. This step led to a reliability factor R = 0.18. The ensuing difference Fourier map revealed an important cloud located around the $z = {}^1/_3$ coordinate, which was unambiguously attributed to copper atoms. At this stage, with the thermal parameters kept isotropic, the refinement on the Mn and Cu site occupancies led to an R factor of 0.10. The strongly anisotropic behavior of copper atoms was set up in the following step of refinement upon introducing the β_{ij} anisotropic thermal factors, whereupon the R factor dropped to 0.05. Full-matrix least-squares techniques including zerovalent scattering factors[16] were used according to Busing.[17] Further correction for secondary

(6) de Meulenaer, J.; Tompa, H. *Acta Crystallogr.* **1965**, *19*, 1014.
(7) Raoux, D.; Petiau, J.; Bondot, P.; Calas, G.; Fontaine, A.; Lagarde, P.; Levitz, P.; Loupias, G.; Sadoc, A. *Rev. Phys. Appl.* **1980**, *15*, 1079.
(8) Michalowicz, A.; Clement, R. *Inorg. Chem.* **1982**, *21*, 3872.
(9) Legros, J. P., unpublished results.
(10) Teo, B. K. In "EXAFS Spectroscopy"; Teo, B. K., Joy, D. C., Eds.; Plenum Press: New York, 1981; pp 13–58 and references therein.
(11) (a) Teo, B. K.; Lee, P. A.; Simons, A. L.; Eisenberger, P.; Kincaid, B. M. *J. Am. Chem. Soc.* **1977**, *99*, 3854. (b) Teo, B. K.; Lee, P. A.; Simons, A. L. *Ibid.* **1977**, *99*, 3856.
(12) (a) Clement, R.; Girerd, J. J.; Morgenstern-Badarau, I. *Inorg. Chem.* **1980**, *19*, 2852. (b) Clement, R.; Audiere, J. P.; Renard, J. P. *Rev. Chim. Miner.* **1982**, *19*, 560.
(13) Mathey, Y.; Clement, R.; Sourisseau, C.; Lucazeau, G. *Inorg. Chem.* **1980**, *19*, 2773.
(14) Mathey, Y.; Clement, R.; Audiere, J. P.; Poizat, O.; Sourisseau, C. *Solid State Ionics* **1983**, *9–10*, 459.
(15) (a) Klingen, W.; Eulenberger, G.; Hahn, H. *Z. Anorg. Allg. Chem.* **1973**, *401*, 97. (b) Brec, R.; Ouvrard, G.; Louisy, A.; Rouxel, J. *Ann. Chim. (Paris)* **1980**, *5*, 499.
(16) "International Tables for X-ray Crystallography"; Kynoch Press: Birmingham, England, 1974; Vol. IV, p 72.

Table II. Interatomic Distances (Å) and Angles (deg) in the $[P_2S_6]$ and $[Mn_{1-x}Cu_{2x}P_2S_6]$ Octahedra[a]

P-P^{vi}	2.196 (3)	P-S(2)	2.024 (1)
P-S(1^{v})	2.023	av	2.023
P(^{vi})-P-S(2)	105.70 (5)	S(1^{v})-P-S(2)	113.09 (5)
P(^{vi})-P-S(1^{v})	105.46 (8)	S(2^{ii})-P-S(2^{vi})	112.92 (8)
Mn-S(1^{i})	2.638 (1)	Mn-S(2^{i})	2.652 (1)
Mn-S(2^{ii})	2.640 (1)	av	2.643
S(1^{v})-S(2)	3.376 (2)	S(2^{i})-S(2^{ii})	3.587 (2)
S(2^{ii})-S(2^{vi})	3.374 (2)	S(1^{i})-S(2^{ii})	3.585 (2)
S(1^{v})-S(2^{ii})	3.818 (2)	S(1^{i})-S(1^{iv})	3.923 (2)
S(2)-S(2^{ii})	3.826 (2)	S(2)-S(2^{i})	3.962 (2)
S(1^{i})-S(2^{i})	3.587 (2)		
Cu-S(1)	2.082 (3)	Cu-S(2^{vii})	2.076 (3)
Cu-S(2)	2.068 (3)	av	2.075
S(1^{i})-Mn-S(2^{ii})	85.56 (5)	S(1^{i})-Mn-S(1^{iv})	96.09 (6)
S(1^{i})-Mn-S(2^{i})	85.39 (5)	S(2)-Mn-S(2^{i})	96.95 (5)
S(1^{ii})-Mn-S(2^{i})	85.34 (5)	S(2^{ii})-Mn-S(1^{iv})	177.09 (3)
S(2^{i})-Mn-S(1^{iv})	92.40 (5)	S(2^{i})-Mn-S(2^{iii})	176.71 (5)
S(2)-Mn-S(2^{ii})	92.89 (6)		
S(1)-Cu-S(2)	119.6 (1)	S(2)-Cu-S(2^{vii})	119.9 (1)
S(1)-Cu-S(2^{vii})	119.1 (2)		

[a] Superscripts indicate equivalent positions as follows: (none) x, y, z; (i) $1/2 - x, -y, 1/2 - z$; (ii) $-x, -y, z$; (iii) $-1/2 + x, y, 1/2 - z$; (iv) $-1/2 + x, y, 1/2 + z$; (v) $1 - x, y, z$; (vi) $-x, -y, -z$; (vii) $1/2 - x, -y, 1/2 + z$.

extinction[18] yielded a conventional $R = 0.041 = \sum[F_o - |F_c|]/\sum F_o$ and $R_w = 0.059 = [\sum w(F_o - |F_c|)^2/\sum wF_o^2]^{1/2}$ with $w = 1/\sigma^2(F)$. The final fractional atomic coordinates and anisotropic and equivalent thermal parameters are given in Table I. Distances and angles (Table II) have been calculated by using ORFFE.[19] The final difference map was featureless except for two peaks (0.13 e Å^{-3}) in $z = 0$ and $z = 1/3$ regions.

All further attempts to improve the picture either by introduction of fractional copper atoms in these two extrapositions or by refinement within noncentrosymmetric space groups were unsuccessful.

Description of the Structure. The structure of $Mn_{0.87}Cu_{0.26}PS_3$ (Figure 1) is clearly related to that of $FePS_3$[15] and $Cr_{1/2}Cu_{1/2}PS_3$.[4] Like these known systems, the title compound has a layered structure built on ABC stacking. An "empty" layer (or van der Waals gap) alternates with a "filled" layer containing phosphorus pairs and manganese and copper atoms. Each cell is made up of two $[P_2S_6]$ and two $[Mn_{1-x}Cu_{2x}S_6]$ octahedra. From the ultimate step of the refinement procedure it turns out that the latter octahedra are occupied simultaneously by 0.85 ± 0.02 Mn in central positions and 2(0.12 ± 0.01) Cu atoms located on two eccentric positions close to the sulfur layer planes. It is clear that the same sulfur octahedron cannot accommodate both the two copper and the manganese atoms even with the above-reported occupancy probabilities. Actually, this picture reflects the disordered distribution of 85 ± 2% $[MnS_6]$ octahedra, very similar to those in the $MnPS_3$ and $FePS_3$ structures, together with 12 ± 1% of a new type of $[S_3Cu\cdots CuS_3]$ octahedra. These percentages compare quite well with the stoichiometric coefficients found by chemical analyses; furthermore, such a disorder can be related to the broadness of the observed reflection spots.

Considering now the metal–sulfur distances extracted from the XRD data analysis (Table II), the Mn–S distances are almost the same (although slightly larger: mean value 2.643 Å) as the corresponding distances of 2.60 Å found in the

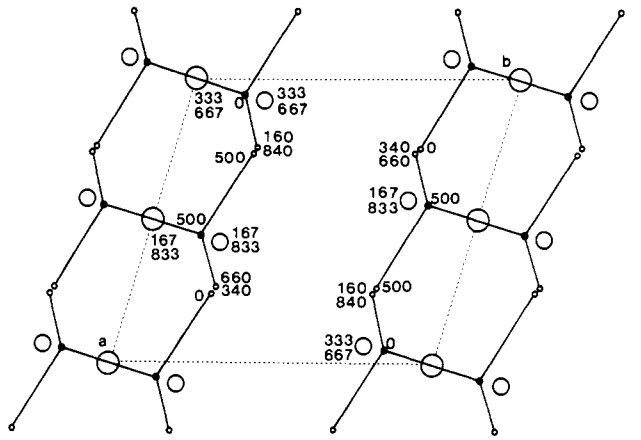

Figure 1. Projection of the structure of $Mn_{1-x}Cu_{2x}PS_3$ (x = 0.13) along [001]. Small, medium, and large open circles indicate sulfur, copper, and manganese positions, respectively. Solid circles indicate phosphorus positions. Numbers represent relative positions (×1000) along the c direction.

$MnPS_3$ compound;[8] it is also clear that the Cu–S distances are correspondingly abnormally short (mean value: 2.075 Å) compared to the expected value;[20-22] this striking feature will be discussed later on. In addition, the two Cu^I ions present a fairly large anisotropic thermal factor in the direction perpendicular to the sulfur plane. The center of the two ellipsoids is located 0.142 (5) Å inside the $[S_3Cu\cdots CuS_3]$ octahedron, and the corresponding intercopper distance is 3.003 (9) Å. These results together with the observation of temperature-dependent low-frequency modes in the Raman spectrum of $Mn_{0.87}Cu_{0.26}PS_3$ strongly suggest that the Cu^I may be responsible for some ionic conductivity.[14] Finally the P–S bond length (Table II) agrees with the values found in any compound of that family, including $FePS_3$ (P–S = 2.030 Å)[15] and $Cr_{1/2}Cu_{1/2}PS_3$ (P–S = 2.034 Å).[4]

EXAFS Results. The $k[\chi(k)]$ spectra of $Mn_{0.87}Cu_{0.26}PS_3$ and of model compounds at both Mn and Cu edges are given in supplementary material. The corresponding radial distribution functions are presented in Figure 2. From these $\tilde{F}(R)$ spectra, several qualitative conclusions are readily accessible: (i) The $Mn_{0.87}Cu_{0.26}PS_3$ spectra at the manganese edge (Figure 2, parts c (300 K) and d (15 K)) show two peaks and seem very similar to those of $MnPS_3$ (Figure 2, parts a (300 K) and b (15 K)). These two peaks and their temperature dependence were already interpreted for the model compound[8] in terms of Mn–S distances (first peak) and of a mixture of Mn–Mn and Mn–P distances (second peak). This similarity indicates that the partial substitution of some Mn^{II} ion by Cu^I ion pairs has not significantly affected the symmetry of the remaining manganese sites since the latter peak has been shown to be sensitive to any change in the local structure (as is shown by its dramatic reduction upon intercalation[8]). (ii) The radial distributions at the copper edge in $Mn_{0.87}Cu_{0.26}PS_3$ (Figure 2, parts g (300 K) and h (15 K)) show an intense first peak and a complex structure above 2.5 Å. The latter structure is strongly temperature dependent. Both modulus and imaginary part of the first peak compare well with those of the Cu–S peak (2.28 Å) of the model compound $K_2Cu(S_2C_2O_2)_2$ (Figure 2, parts e (300 K) and f (15 K)); as the shifts in the Cu–S distances between the unknown and the model compounds are smaller than 0.1 Å, a first estimate of these distances in the title compound is 2.19–2.20 Å. (iii) The set of irreducible differences observed between the spectra of $Mn_{0.87}Cu_{0.26}PS_3$ at Mn and Cu edges (metal–sulfur distances, higher distance contributions, and temperature dependence) strongly supports the diagnosis of two distinct environments for Mn and Cu ions. Consequently, any occupancy of the Mn^{II} vacancies at the

(17) Busing, W. R. *Acta Crystallogr., Sect. A: Cryst. Phys., Diffr., Theor. Gen. Crystallogr.* **1971**, *A27*, 683.
(18) Becker, P.; Coppens, P. *Acta Crystallogr., Sect. A: Cryst. Phys., Diffr., Theor. Gen. Crystallogr.* **1974**, *A30*, 129, 148.
(19) Busing, W. R.; Martin, K. O.; Levy, H. A. *Oak Ridge Natl. Lab. [Rep.], ORNL-TM (U.S.)* **1964**, *ORNL-TM 306*.

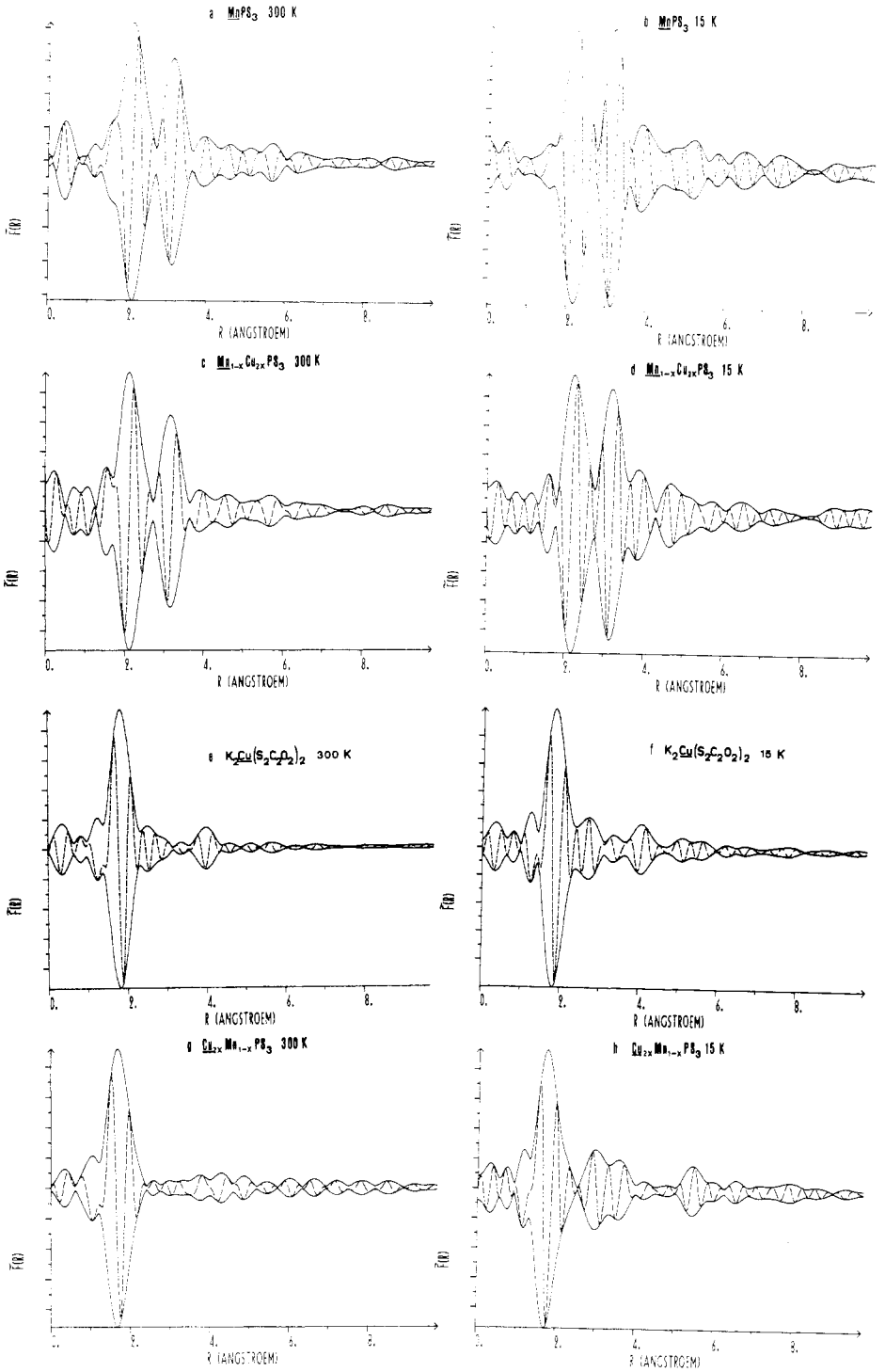

Figure 2. EXAFS radial distribution functions $\tilde{F}(R)$ = FT $\{k^3[\chi(k)]\}$ of $Mn_{1-x}Cu_{2x}PS_3$ (x = 0.13) (traces c, d, g, h) and of the two model compounds $MnPS_3$ (traces a, b) and $K_2Cu(S_2C_2O_2)_2$ (traces e, f). Results at 15 and 300 K are given for both Mn and Cu edges (the absorbing metal is underlined in the formula): (—) $\pm|\tilde{F}(R)|$ (the modulus of the Fourier transform); (---) Im $[\tilde{F}(R)]$ (the imaginary part of the Fourier transform).

Table III. Three-Shell Fits (in Two Steps) of EXAFS Spectra at the Mn Edge[c]

		Mn-S		Mn-P		Mn-Mn[a]		
compd	T, K	σ, Å	R, Å	σ, Å	R, Å	σ, Å	R, Å	%ρ[b]
$Mn$$PS_3$	300	0.08	2.58	0.08	3.66	0.08	3.50	1.8
	15	0.05	2.60	0.02	3.66	0.02	3.49	1.6
$Mn_{0.87}Cu_{0.26}PS_3$	300	0.08	2.59	0.08	3.66	0.08	3.51	1.5
	15	0.05	2.61	0.02	3.65	0.02	3.51	1.3

[a] Slight differences are observed between these values and those previously published;[8] this is due to the use of an improved program allowing the fitting of a single value for two parameters, namely the two σ values of the second peak. [b] $\rho = \Sigma_{k(\min)}^{k(\max)}(\chi_{exptl} - \chi_{th})^2 k^5 / \Sigma_{k(\min)}^{k(\max)}\chi_{exptl}^2$. k^5 is the residual factor. [c] The corresponding figures are given in the supplementary material. $k(\min) = 3$ Å^{-1}; $k(\max) = 11$ Å^{-1}.

Table IV. Single-Shell Fits of EXAFS Spectra at the Cu Edge[b]

compd	T, K	Cu–S σ, Å	R, Å	%ρ
$K_2Cu(S_2C_2O_2)_2$	300	0.07	2.28[a]	1.5
	15	0.05	2.28	1.9
$Mn_{0.87}Cu_{0.26}PS_3$	300	0.08	2.21	2
	15	0.06	2.22	2.5

[a] d_{XRD}(Cu–S) = 2.28 Å.[9] [b] The corresponding figures are given in the supplementary material.

Table V. Metal–Sulfur Distances As Obtained by the Two Methods[a]

M–S	XRD dist, Å	EXAFS dist, Å
Cu–S	2.075 ± 0.007	2.22 ± 0.02
Mn–S	2.643 ± 0.009	2.61 ± 0.02

[a] The EXAFS values are those obtained at 15 K since the thermal vibration distance distribution at 300 K is responsible for a systematic error of −0.01 to −0.02 Å.[8]

center of the sulfur octahedra by a significant amount of Cu^I ions can be definitely ruled out. Tables III and IV summarize the least-squares fitting results for the Mn and the Cu edge, respectively. Only the first shell was fitted in the latter case, while as previously done on $MnPS_3$,[8] a two-step fit over three shells has been performed and has proved satisfactory. The Mn–S, Mn–Mn, and Mn–P distances are in excellent agreement with the values Mn–S = 2.59 Å, Mn–Mn = 3.52 Å, and Mn–P = 3.68 Å calculated for $MnPS_3$ from powder X-ray diffraction data by assuming a structural isomorphism with $FePS_3$.[15] As qualitatively discussed above, these results nicely confirm that in $Mn_{0.87}Cu_{0.26}PS_3$ the Mn site is very similar to the Mn site in the model compound. Also, the Cu–S distance fitted at 2.22 Å in $Mn_{0.87}Cu_{0.26}PS_3$ is very close to the first qualitative estimate. Nevertheless, in order to prevent any error due to a fit on a false minimum, several attempts using different R_{Cu-S} and E_0 starting values in the ranges 2.05–2.35 Å and 8970–9000 eV were also carried out. Surprisingly enough, it was impossible to find any refinement of the EXAFS data leading to a Cu–S distance close to the "crystallographic" value of 2.07 Å proposed in the above XRD section.

In other respects, all attempts to identify the nature of and to fit the outer peaks have failed: these contributions to the EXAFS spectrum probably arise from too many types of atoms with too complex a distribution of distances to allow a detailed EXAFS analysis. An unambiguous location of the Cu^I ion in the $Mn_{0.87}PS_3$ framework is therefore impossible from the EXAFS data only.

Discussion

The metal–sulfur distances obtained either by XRD experiments or by EXAFS measurements at both Mn and Cu edges are given in Table V. Besides a small deviation (~0.03 Å) between the two Mn–S distances with d_{XRD}(Mn–S) > d_{EXAFS}(Mn–S), a large inconsistency between the two Cu–S distances with d_{XRD}(Cu–S) << d_{EXAFS}(Cu–S) is obvious. The origin of this enormous discrepancy (almost 0.15 Å) was investigated with very careful consideration of each stage of the experimental procedures and data analyses; but no step, neither in XRD nor in EXAFS, could be incriminated to account for this difference. However, upon consideration of the usual range of experimental values for such Cu^I–S linkages[20-22] on the one hand and the sum of the covalent radii $r_{Cu} + r_S$ = 1.35 + 1.04 = 2.39 Å[23] on the other, it is clear that the EXAFS distance is much more likely to be correct. Moreover, as this result is obtained by assuming a Gaussian distribution of the Cu–S distances, it could be slightly shorter than the true averaged value if the distribution is asymmetric (even at 15 K if this distribution is partially static).[24] Notwithstanding, its use within the XRD structural picture produces a series of other inconsistencies and obviously no settlement of the problem will be achieved by following this course.

Although less apparent than the preceding contradiction, another serious divergence lies between the Cu···Cu XRD distance (3.003 Å) and the EXAFS data. At 15 K such a distance should correspond to a peak in the radial distribution function $F(R)$ of the EXAFS spectrum at the Cu edge. If we assume that the second peak of the experimental spectrum (Figure 2h) located at ~2.9 Å represents this Cu···Cu contribution, the true copper–copper distance should be expected in the 3.2–3.3-Å range since a shift of 0.3–0.4 Å is known to occur between the observed position of a Cu···Cu peak and the true corresponding distance.[25] Obviously an important overlap between the Cu···Cu peak and some Cu–S and Cu–P contributions (see Figure 2h) precludes a more precise location through filtering and single-shell curve fitting, but again this EXAFS estimation apparently contradicts the XRD results. Moreover, neither the first contradiction above depicted (Cu–S distances) nor the second one (Cu···Cu distances) can be overcome by changing only the Cu^I ion positions in the $Mn_{0.87}PS_3$ framework determined by XRD. If, for instance, the Cu–S distances are changed from 2.075 to 2.22 Å, a copper to sulfur plane distance of about 0.8 Å (since $S(1^i)$–$S(2^i)$ = $S(2^i)$–$S(2^{ii})$ 3.587 Å) (Table II) is obtained. With use of this value and for obvious reasons of steric hindrance, the two Cu^I ions cannot coexist inside the $[S_3Cu\cdots CuS_3]$ octahedron described in the above XRD section.[26] All these divergences set a very puzzling problem whose solution arose from the following basic ideas:

(i) It is not surprising to observe inconsistency between sets of data obtained by methods based on drastically different principles. On the one hand, XRD assumes the existence of a long-range order and gives information averaged over all the unit cells of the crystal under study. This leads first to a crude and unrealistic description of the structure with indistinguishable $[Mn_{1-x}Cu_{2x}S_6]$ octahedra, interpreted upon further considerations by means of a disordered distribution of $[MnS_6]$ and $[S_3Cu\cdots CuS_3]$ distinct octahedra. On the other hand, EXAFS leads directly (and because of its sensitivity to the short-range order only) to the Cu and Mn ion local environments. These determinations, locally averaged when large distance distributions occur, are independent of the parameters of the unit cell, of the stoichiometry, and thus of the percentages of each kind of octahedra. In other respects, EXAFS is unable to give a picture of the complete structure.

(ii) There is no "a priori" reason for expecting identical sizes in the S_6 skeletons of the $[MnS_6]$ and $[S_3Cu\cdots CuS_3]$ octahedra. Actually the XRD experiment averages not only the atomic content of each octahedron but also its dimensions, yielding finally "indistinguishable" entities where "distinguishable" ones do coexist. Clearly, the distinction between these two kinds of octahedra with their true (unaveraged) dimensions would have been inaccessible without the EXAFS data; meanwhile no correct description of the copper environment and "a

(20) Brown, D. B.; Zubieta, J. A.; Vella, P. A.; Wrobelski, J. T.; Watt, T.; Hatfield, W. E.; Day, P. *Inorg. Chem.* **1980**, *19*, 1945.
(21) Eller, P. G.; Corfield, P. W. *J. Chem. Soc., Chem. Commun.* **1971**, 105.
(22) Siiman, O. *Inorg. Chem.* **1981**, *20*, 2285.
(23) Pauling, L. In "The Nature of the Chemical Bond", 3rd ed.; Cornell University Press: Ithaca, NY, 1967; p 246.
(24) Eisenberger, P.; Brown, G. S. *Solid State Commun.* **1979**, *29*, 481.
(25) Martens, G.; Rabe, P.; Schwentner, N.; Werner, A. *Phys. Rev. B: Condens. Matter* **1978**, *17*, 1481.
(26) Michalowicz, A.; Vlaic, G.; Clement, R.; Mathey, Y. In "Proceedings of the International Conference on EXAFS and Near Edge Spectroscopy"; Springer-Verlag: West Berlin, 1983; p 222.

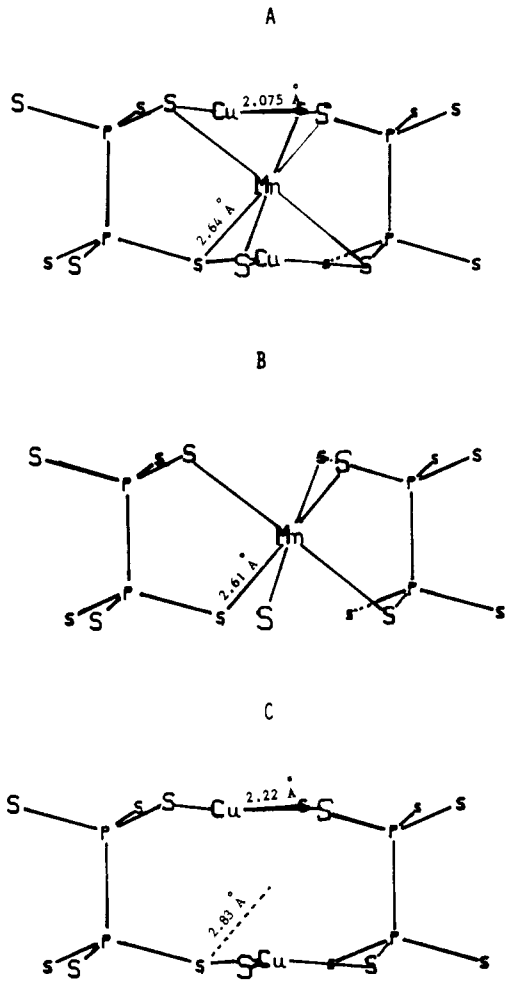

Figure 3. Schematic representations of the Mn and Cu sites in $Mn_{1-x}Cu_{2x}PS_3$ ($x = 0.13$): (A) XRD-averaged site; (B) manganese site; (C) copper site. The center-to-sulfur distance of 2.83 Å is calculated with the assumption that the three types of sites $[MnS_6]$, XRD-averaged octahedron, and $[S_3Cu\cdots CuS_3]$ are homothetic.

fortiori" no correct description of the whole structure would have been reached without the XRD data. The dimensions and the atomic arrangements of the two distinct octahedra are compared with those averaged by XRD in Figure 3. The presence of two Cu^I ions in 13% of the octahedra (Figure 3c) induces an expansion of these latter with respect to the 87% of more classic $[MnS_6]$ octahedra (Figure 3B). This relative dilatation is responsible for the weak but significant increase (0.03 Å) observed on the Mn–S distances upon averaging the center-to-apex distances over the totality of the octahedra. Assuming that a homothetic relationship links the three octahedra under consideration in Figure 3, these center-to-apex distances turn out to be 2.643 (2.22/2.075) = 2.83 ± 0.04 Å in $[S_3Cu\cdots CuS_3]$ (see Table V and Figure 3C). Correspondingly, as 87% of the octahedra are smaller (Figure 3) than the $[S_3Cu\cdots CuS_3]$ ones, the Cu–S distances drop dramatically from their local EXAFS value of 2.22 Å (Figure 3C) to the abnormally short XRD-averaged value 2.075 Å (Figure 3A).

Considering now the last kind of pseudooctahedron in the structure, namely the $[S_3PPS_3]$ entity, its local dimensions slightly depend on the size of its neighboring $[MnS_6]$ and/or $[S_3Cu\cdots CuS_3]$ entities with which it shares sulfur atoms.

In that case the conjunction of XRD and EXAFS measurements fails in resolving the problem of the distribution of these different $[S_3PPS_3]$ entities and does not allow us to determine their true dimensions. All these pseudooctahedra indeed have the same atomic content and therefore both methods will give averaged information. Consequently an EXAFS experiment carried out at the phosphorus edge would be worthless.

Turning back to the problem of the Cu···Cu distance within the $[S_3Cu\cdots CuS_3]$ entities, a simple calculation based again on an homothetic correspondence between XRD-averaged (Figure 3A) and EXAFS (Figure 3C) octahedra gives a value of 3.003(2.22/2.075) = 3.21 Å, which compares well with the EXAFS estimation.

Therefore, as far as Mn or Cu environments are concerned, the apparent "mismatch" between XRD and EXAFS data for the $Mn_{0.87}Cu_{0.26}PS_3$ compound appears to be understood. Still better, if it is overcome in spite of the disorder existing among the distinct octahedra, a quite detailed description of each metallic site becomes accessible. With the knowledge that disorder exists in a wide variety of solids, such a positive result deserves to be underlined. As a matter of fact many XRD structural determinations are likely to be only qualitatively correct since XRD averaging over several kinds of sites could have led to erroneous distances.

Clearly a much better insight into the structure of disordered solids could be expected if (i) the disorder occurs over a reasonable number of sites, (ii) each kind of site is associated with a particular type of atom, and (iii) in complement to XRD study and as a probe of the local environment for each kind of site, EXAFS measurements can be performed at the corresponding edges.

Such a new approach was recently experienced in the case of the $KCl_{1-x}Br_x$ systems.[27] In these solid solutions, the two distinct sites are isomorphous but the lattice relaxation around the dilute bromide ion is inaccessible through XRD only. EXAFS measurements performed at the Br edge were reported to differ by 0.06–0.08 Å from the XRD-averaged values and have led readily to the magnitude of the relaxation. However, the informative power of the XRD and EXAFS methods when used in conjunction is still better illustrated by the present results on $Mn_{0.87}Cu_{0.26}PS_3$ compound, where both distinct atomic contents and distinct site geometries exist and are satisfactorily described.

Acknowledgment. We thank the staff of the linear accelerator laboratory of Orsay, France, who operated the storage ring DCI for the synchrotron radiation dedicated shift used in this work. We also thank the staff of LURE, particularly those involved in the EXAFS spectrometer design. We are grateful to Dr. J. Goulon for his help in writing the EXAFS analysis program, to Prof. N. Rodier for his help in XRD data collection, and to Dr. J. Grimbot for the XPS and Auger spectra recording and interpretation. Finally it is a pleasure to thank Prof. P. Khodadad, Prof. R. Fourme, Dr. C. Sourisseau, and Dr. R. Clement for helpful discussions.

Supplementary Material Available: A listing of observed and calculated structure factors, room-temperature and 15 K $k[\chi(k)]$ spectra of $Mn_{0.87}Cu_{0.26}PS_3$, $MnPS_3$, and $K_2Cu(S_2C_2O_2)_2$ at both Mn and Cu edges, and fits of the filtered EXAFS data of $Mn_{0.87}Cu_{0.26}PS_3$ at both Mn and Cu edges (14 pages). Ordering information is given on any current masthead page.

(27) Murata, T.; Lagarde, P.; Fontaine, A.; Raoux, D. In "Proceedings of the International Conference on EXAFS and Near Edge Spectroscopy"; Springer-Verlag: West Berlin, 1983; p 271.
(28) $\mu x = \ln (I_0/I)$ calculated by using: McMaster, W. H.; Kerr Del Grande, No.; Mallett, J. H.; Hubbell, J. H. "Compilation of X-ray Cross-Sections"; National Bureau of Standards: Washington, DC; UCRC-50174, Section II, Rev. 1.
(29) Stern, E. A.; Heald, S. M. In "Handbook on Synchrotron Radiation"; Koch, E. E., Ed.; North-Holland Publishing Co.: Amsterdam, 1983; pp 955–1014.